

An effective histogram-based approach to JPEG-100 forensics

Anh Thu Phan Ho, Kai Wang and François Cayre

Univ. Grenoble Alpes, GIPSA-Lab, F-38000 Grenoble, France

CNRS, GIPSA-Lab, F-38000 Grenoble, France

e-mail: {anh-thu.phan-ho, kai.wang, francois.cayre}@gipsa-lab.grenoble-inp.fr

Abstract— This paper proposes an improved histogram-based approach to identifying whether an image is never compressed or has undergone JPEG compression with quality factor 100. The key idea is that the image's DCT (Discrete Cosine Transform) coefficients follow either of two families of parametric distributions, corresponding respectively to never compressed images and JPEG-100 compressed ones. This paper highlights that choosing the generalized Gaussian distribution (GGD) to model the DCT coefficients and constructing a DCT histogram with precision higher than integer create a prominent distinction between the DCT coefficients distribution of the two kinds of images. Experiments demonstrate that the proposed approach significantly outperforms existing histogram-based methods for the task of JPEG-100 forensics.

Keywords— JPEG-100 forensics, DCT histogram, generalized Gaussian distribution, histogram fitting.

I. INTRODUCTION

Over past decades, the wide variety of powerful digital image processing tools has made it simpler and easier to tamper with an image while leaving no obvious visual clue. Therefore, insuring the authenticity of an image is of paramount importance. There has been accordingly an increasing interest in digital image forensics research. An important forensic problem is to identify whether an image is never compressed or has undergone JPEG compression, one of the most popular lossy image compression standards. In general, JPEG forensics aims at exposing the compression history of a given image, and it can be a useful tool to assist tasks such as determining the image origin (*i.e.*, identifying the digital camera and/or the image editing software used to generate/save the image) [1] and detecting image forgeries [2]. Considerable efforts have been devoted to JPEG forensics research in past decades [3], [4], [5], [6], [7]. However, exposing JPEG compression with very high quality factor is still a challenging problem, and in the meanwhile such high-quality JPEG compression is commonly used in digital cameras and can be involved in the creation of tampered images [4].

Two main approaches to JPEG compression detection are recompression-based and DCT (Discrete Cosine Transform) histogram-based. The basic idea of the first kind of approach is to perform JPEG recompression of the given image to gain more information about it for forensic purposes [4], [5], [6]. Discriminative features for JPEG forensics can be derived based on information gathered from recompression, such as image block stability [4] and the level of quantization

noise in multiple compression cycles [5], [6]. The second kind of approach is based on investigating histogram of DCT coefficients constructed with integers as histogram bin centers [3], [7]. In [3], Fan and de Queiroz assumed that the AC DCT coefficients follow Laplacian distribution, then they estimated each step q (an integer) of the JPEG quantization table by utilizing maximum likelihood estimation. If the step q of a given DCT subband was estimated to be 1, the method in [3] claimed that this subband was never compressed. In the state-of-the-art histogram-based method from Luo et al. [7], the authors constructed a statistic test based on the percentage of the AC coefficients on their two specific ranges, *i.e.*, within $(-1, 1)$ and within $(-2, -1) \cup [1, 2)$, to discriminate the original and the compressed image. Unfortunately, existing histogram-based methods [3], [7] in general fail for the task of JPEG-100 forensics (*i.e.*, exposing JPEG compression with quality factor 100, where all quantization steps are equal to 1), while recompression-based methods can provide satisfying results [4], [5], [6]. Figure 1 illustrates the difficulty of JPEG-100 forensics, especially for histogram-based methods. We can see that the original UCID00001 [8] image and the corresponding JPEG-100 compressed version look nearly identical, even when they are zoomed in. Moreover, their DCT histograms, constructed with the bin width equal to 1, are also very similar. One can argue that the peak at 0 decreases a little after JPEG-100 compression, however in practice this cannot be used as a forensic feature because of the variety of uncompressed images, *i.e.*, we can easily find another uncompressed image with similar peak height as that of the JPEG-100 compressed UCID00001 image shown in Fig. 1.

Our objective in this paper is to improve the JPEG-100 forensics performance of DCT histogram-based method so that it can be as competitive as the approach based on recompression. Indeed, we believe that, as opposed to recompression-based methods, we can already gain enough discriminative information only from the DCT coefficients histogram of a given image, to expose the intrinsic trace of JPEG compression even with quantization step $q = 1$. This is because, as shown later, DCT coefficients before and after JPEG compression have quite different distributions, and this difference can be easily exposed in a properly constructed DCT histogram, in particular with histogram bin width smaller than integer. Experimental results show that our proposed method significantly outperforms existing histogram-based methods in identifying

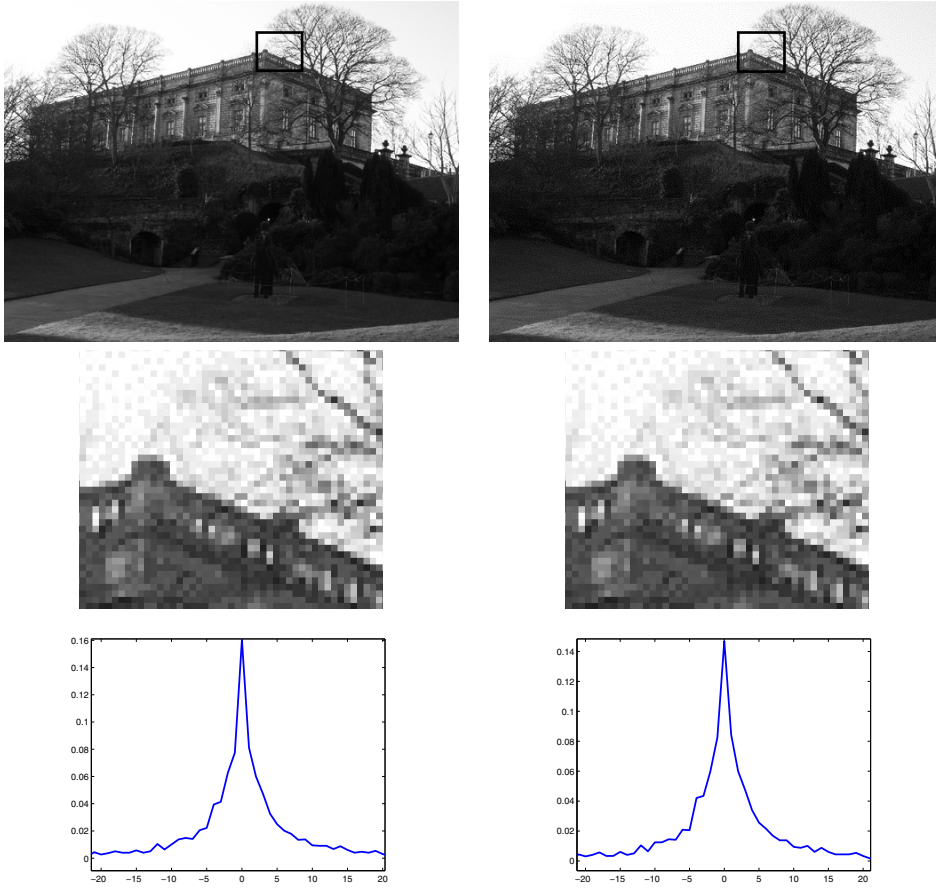


Fig. 1. The uncompressed UCID00001 image (first row, left) and its JPEG-100 compressed version (first row, right) look nearly identical, even for their close-ups (second row). The DCT histograms of subband (4, 4) of these two images, constructed with bin width $w = 1$, are also very similar (third row).

whether an image is originally uncompressed or has been JPEG compressed with quality factor 100.

The remainder of this paper is organized as follows. Section II presents our formulation of the research problem as well as the two possible distribution families of DCT coefficients. In Section III, we first present how we come up with the idea of histogram fitting and histogram construction and then sketch the proposed method. The experimental results are shown in Section V. Finally the conclusion and future work are drawn in Section VI.

II. PROBLEM FORMULATION

To discriminate the original, uncompressed image I from the JPEG compressed image J , we study the histograms of their DCT coefficients D_I and Y^* .

$$I \xrightarrow{\text{DCT}} D_I \quad (1)$$

$$J \xrightarrow{\text{DCT}} Y^*. \quad (2)$$

The goal of this phase is to analyze the distributions of D_I and Y^* and to present the general idea to conduct JPEG forensics based on these two distributions. It is worth noting that the analysis in this section is true for any quantization

step q . Therefore, it is possible to use this framework for general-purpose JPEG forensics of any quality factor though our current objective is to do forensics on JPEG 100 ($q = 1$).

In JPEG encoding, before being transformed into DCT domain, images are first splitted into nonoverlapping 8×8 pixel value blocks. After the transformation, in each DCT block there are 64 coefficients denoted as C_{mn} , where $m, n \in \{1, \dots, 8\}$. We define a DCT subband (m, n) as a set of all C_{mn} coefficients with fixed m, n values from all blocks. In this paper, we only consider AC coefficients, *i.e.*, subbands (m, n) with $(m, n) \neq (1, 1)$.

A key idea is that, the distribution of each AC subband D_I follows the GGD (generalized Gaussian distribution) while that of AC subband Y^* follows the perturbed “discrete” GGD which will be defined in Section II-B. Basing on this observation, we make a distinction between I and J .

In the following subsections, we give more details on the distribution of D_I and Y^* .

A. Distribution of D_I

There have been several probabilistic models proposed for the distribution of DCT coefficients for natural images such as Gaussian distribution, Laplacian, Cauchy, GGD, etc [9],

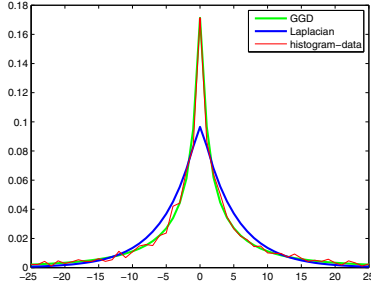


Fig. 2. DCT coefficients histogram of subband (4,4) of the image UCID00001 [8] along with the best fitting GGD and Laplacian distribution.

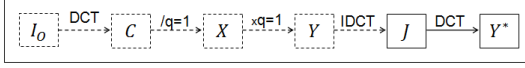


Fig. 3. JPEG-100 processing pipeline (part with dashed segments). After IDCT (inverse DCT), attackers may save the decompressed image as a bitmap in a lossless format as J . Forensic analysis is carried out on Y^* , DCT coefficients of J .

[10]. Nearly all of existing works on image forensics and anti-forensics use Laplacian as a distribution of DCT coefficients for AC subband [3], [11], [12]. However, GGD fits better the distribution of AC coefficients since GGD is a parametric family of distribution including Laplacian as a special case, see Fig. 2. Therefore we assume that AC coefficients of the never compressed image follow the GGD which is defined as

$$p(x; \alpha, \beta) = \frac{\beta}{2\alpha\Gamma(1/\beta)} e^{-(|x|/\alpha)^\beta} \quad (3)$$

where $\Gamma(\cdot)$ is the Gamma function, *i.e.*, $\Gamma(z) = \int_0^\infty e^{-t} t^{z-1} dt, z > 0$.

B. Distribution of Y^*

In digital image forensics, J is a JPEG compressed image saved in a lossless format. J must have been compressed from some original image denoted by I_0 , see Fig. 3. I_0 is transformed into DCT coefficients C_{mn} which are then quantized using the quantization steps q_{mn} , to obtain the quantized coefficients $X_{mn} = \text{round}\left(\frac{C_{mn}}{q_{mn}}\right)$. In the dequantization stage, we have the dequantization coefficient Y_{mn} being a multiple of the step q_{mn} , $Y_{mn} = k_{mn}q_{mn}$. However, in reality what we can observe and work on is not exactly Y_{mn} but its perturbed version Y_{mn}^* because of the rounding and truncation errors in the pixel value domain. These errors are introduced when saving image in a lossless format comprising a matrix of integer pixel values (the saved image is actually J in our notation, see Fig. 3). In [3], the error between Y_{mn} and its perturbed version Y_{mn}^* is theoretically bounded by B_{mn} :

$$|Y_{mn}^* - Y_{mn}| \leq B_{mn} \quad (4)$$

where B_{mn} is define as in [3].

As mentioned above, after the quantization stage, the DCT coefficients Y_{mn} are discretized and $Y_{mn} = k_{mn}q_{mn}$ thus Y_{mn} is governed by the discrete GGD, see Fig. 4 (a), which is formulated as follows:

$$p_Y(Y_{mn} = kq_{mn}; \alpha, \beta) = \int_{kq - \frac{q}{2}}^{kq + \frac{q}{2}} p(y; \alpha, \beta) dy \quad (5)$$

where $p(y; \alpha, \beta)$ is the GGD probability density function of DCT coefficients C_{mn} before quantization.

The probability of Y_{mn}^* given q_{mn}, α, β is computed as follows:

$$\begin{aligned} p(Y_{mn}^*; q_{mn}, \alpha, \beta) &= \sum_y p(Y_{mn}^* = y; q_{mn}, \alpha, \beta) \\ &= \sum_{k: |Y_{mn}^* - kq_{mn}| \leq B_{mn}} p_{Y^*|Y}(Y_{mn}^* | Y = kq_{mn}; q_{mn}, \alpha, \beta) \times \\ & p_Y(kq_{mn}; q_{mn}, \alpha, \beta) \\ &= \sum_{k: |Y_{mn}^* - kq_{mn}| \leq B_{mn}} p_{Y^*|Y}(Y^* | Y = kq_{mn}) p_Y(kq_{mn}; q_{mn}, \alpha, \beta), \end{aligned} \quad (6)$$

where $p_{Y^*|Y}(Y^* | Y = kq_{mn})$ follows the modified Gaussian distribution [3] as following:

$$\begin{aligned} p_{Y^*|Y}(Y^* | Y = kq_{mn}) &= \begin{cases} 0 & \text{if } |Y^* - Y| > B_{mn}, \\ \frac{\exp\left[-6(Y - Y^*)^2\right]}{Z} & \text{else,} \end{cases} \quad (7) \end{aligned}$$

where Z is a normalizing constant.

The distribution $p(Y^*; q_{mn}, \alpha, \beta)$ defined in (6) is a perturbed version of Y since loosely speaking, it is created from Y by multiplying it with a so-called bump function $p_{Y^*|Y}(Y^* | Y = kq_{mn})$. Therefore in Fig. 4 we see that each bump of distribution Y^* is made from the corresponding discrete line of distribution of Y . That is why we call the distribution of Y^* as perturbed “discrete” GGD but it is actually a continuous distribution.

C. General idea

After modeling the distribution of subband D_I and that of subband Y^* , we present the general idea on how to perform JPEG forensics with it.

We have two families of parametric distributions GGD and perturbed “discrete” GGD. For given data, we estimate the best parameters of each family so that we have the “best” fitting candidate distribution from each family. We then measure the “goodness of fit” for each of two aforementioned candidates

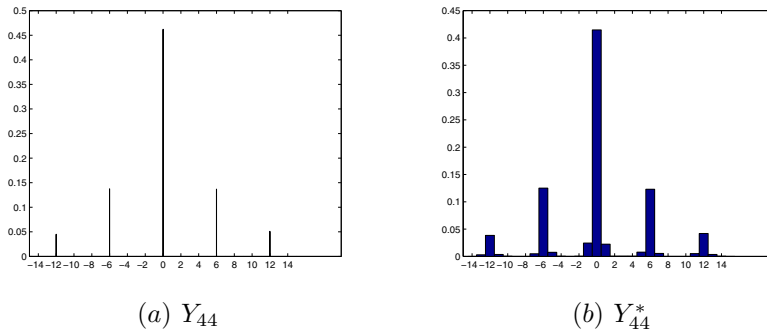


Fig. 4. Histogram of Y_{44} and Y_{44}^* of the image UCID00001 compressed at quantization step $q_{44} = 6$.

to make the final decision about which family better describes the given data. It should be noted that the same measurement of goodness of fit has to be used throughout the whole process of the best parameter estimation for both kinds of distribution and their comparison, so as to ensure the reliability of the final decision. In the next section, we present our JPEG-100 forensic method which puts this idea in practice.

III. PROPOSED METHOD

As discussed in previous section, we need to find the best parameters of each family distribution to have the best fitting. The maximum likelihood method is a natural choice to estimate the parameters. However, in our problem, the distribution of Y^* , perturbed “discrete” GGD is very complicated to deal with using maximum likelihood estimation even numerically, since we frequently encounter the problem of local minima during the optimization. This complexity would also be the reason why existing forensic methods avoid the problem formulation with GGD and resort to tractable distributions such as Laplacian. We have finally adopted an alternative solution by estimating parameters via histogram fitting and using fitting error as a measure of goodness of fit. This method is quite effective due to its simplicity and reasonable goodness of fit result as shown later in Section V.

A key element of histogram fitting method is to construct an appropriate histogram which is discussed in the next subsection.

A. Histogram construction

A histogram requires three parameters: the number of bins denoted by n_b , the bin width denoted by w , and the range $R = [R_1, R_2]$.

The i^{th} bin of histogram h is defined as:

$$I_i = [R_1 + (i - 1)w, R_1 + iw). \quad (8)$$

The central point x_{ic} of each interval I_i is defined as:

$$x_{ic} = R_1 + (i - 1)w + \frac{w}{2}. \quad (9)$$

Since we assume that the DCT coefficients follow the GGD with mean equal to zero, we thus choose the range R and n_b

such that zero is one of central points. Particularly, we choose n_b as an odd number and range R as follows:

$$R = \left[-\frac{n_b}{2} \times w, \frac{n_b}{2} \times w \right). \quad (10)$$

Choosing an appropriate bin width w plays a decisive role in our method. All of existing DCT histogram-based methods construct histogram with the bin width equal to 1 which fails to identify JPEG-100 images [3], [7]. It appears unfeasible both visually and computationally to make any distinction between the never compressed and the JPEG-100 image when using the histograms constructed with the bin width $w = 1$ (cf. Fig. 1, bottom row). Therefore, in order to overcome this problem, we propose to construct a histogram with bin width $w = 0.5$ which can expose prominently the artifact of JPEG-100. In Fig. 5, the distribution of the DCT coefficients of natural image D_I tends to be “smooth” while that of JPEG compressed image Y^* tends to have zigzag shape since the occurrence of DCT coefficients concentrates around the positions which are the multiple of quantization step $q = 1$.

There are many possible distance measures between two histograms. The readers can find a good categorization of these measures in [13]. We compute fitting error using measures including norm-1 error, norm-2 error and Kullback-Leibler divergence. Experimental results show that norm-1 error performs the best in terms of histogram fitting and forensic analysis. Hence we utilize the norm-1 error to measure the bin to bin distance of two normalized histograms h and \hat{h} :

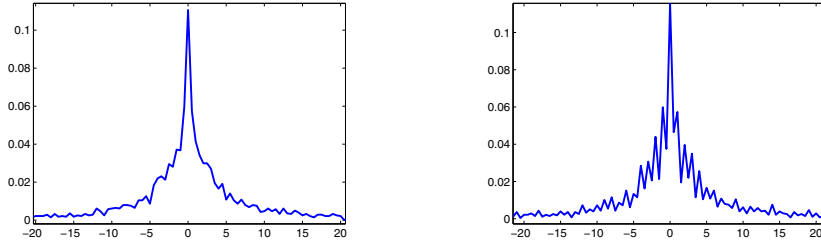
$$d(h, \hat{h}) = \sum_{i=1}^{n_b} |h_i - \hat{h}_i|. \quad (11)$$

IV. FORENSIC METHOD

Our JPEG-100 forensic method is summarized as follows:

- Given the DCT coefficients of a subband of an image, we extract a histogram h .
- We denote by $h_{D_I}(\alpha, \beta)$ a histogram constructed from the GGD defined in Eq. (3) and find the best fitting histogram to h as follows:

$$\hat{h}_{D_I}(\hat{\alpha}, \hat{\beta}) = \arg \min_{\alpha, \beta > 0} d(h_{D_I}(\alpha, \beta), h). \quad (12)$$



(a) Histogram of D_I , bin width $w = 0.5$ (b) Histogram of Y^* , bin width $w = 0.5$

Fig. 5. DCT histogram of subband (4, 4) of never compressed image UCID00001 and its JPEG-100 compressed version with bin width $w = 0.5$.

- We denote by $h_{Y^*}(\alpha, \beta, q = 1)$ a histogram constructed from the perturbed “discrete” GGD defined in Eq. (6). and find the best fitting histogram to h as follows:

$$\hat{h}_{Y^*}(\hat{\alpha}^*, \hat{\beta}^*, q = 1) = \arg \min_{\alpha, \beta > 0} d(h_{Y^*}(\alpha, \beta, q = 1), h). \quad (13)$$

- If $d(\hat{h}_{D_I}, h) \leq d(\hat{h}_{Y^*}, h)$ we say the given subband is never compressed. Otherwise, the given subband is JPEG-100 compressed.

V. EXPERIMENTAL RESULTS

In order to validate the proposed JPEG-100 forensic method we conduct experiments on 5 subbands from low to high frequency (2, 2), (4, 4), (5, 5), (6, 6), (8, 8) of 1338 uncompressed grayscale images¹ from the UCID database [8] and their 1338 corresponding JPEG-100 images which are compressed using the Matlab function `imwrite`. In all our experiments, the DCT histogram is extracted with parameters $n_b = 51$, $w = 0.5$, $R = [-12.75, 12.75]$ (see Section III-A). The range $R = [-12.75, 12.75]$ is good enough to get confident forensic results since most of the values of the coefficients concentrate around this interval.

We solve Eqs. (12) and (13) by an interior point based algorithm using the Matlab optimization Toolbox. Fig. 6 gives an example to show the effectiveness of the proposed forensic method. Fig. 6 (a) depicts the DCT histogram of the subband (4, 4) from the never compressed UCID00001 image and its best fitting histograms of GGD and perturbed “discrete” GGD. The norm-1 fitting error of GGD (0.112) is much lower than that of the perturbed “discrete” GGD (0.265). This is a desired result which gives correct forensic decision according to the decision rule given at the end of Section III. Similarly, Fig. 6 (b) depicts the DCT histogram of the subband (4, 4) from the JPEG-100 compressed version of UCID00001 and the corresponding two best fitting histograms. As expected, perturbed “discrete” GGD has a lower fitting error than GGD (with norm-1 errors 0.123 vs. 0.294), suggesting that the given subband comes from a JPEG-100 image.

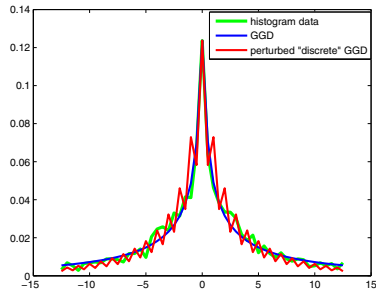
To further demonstrate the effectiveness of our method, we compare it to the Fan’s method [3] and the Luo’s method [7],

¹The original color images in UCID database are converted into 8-bit grayscale images using the Matlab function `rgb2gray` before being tested.

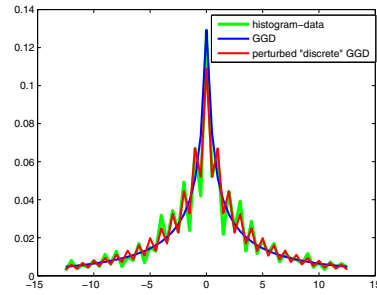
most effective DCT histogram-based JPEG forensic methods proposed so far. Not only comparing with their original results, we also make a comparison with their improved version by using the histogram with the bin width 0.5. To have a detailed and fair comparison, we compute the accuracy rate of all the compared methods for each subband. The accuracy rate is computed as the sum of the number of correctly classified natural and JPEG-100 images, over the total number of samples ($2 \times 1338 = 2678$ images). The accuracy rate of Luo’s method is computed based on the comparison between a scalar feature and a threshold. The threshold is chosen in such a way that it gives the best classification on the tested images.

Table 1 presents the classification accuracy of our method (last column) and the four compared histogram-based methods. It can be observed that our method significantly outperforms the other four methods. Fan’s original method actually provides random guess when identifying never compressed and JPEG-100 images. Even with the new histogram with bin width equal to 0.5, Fan’s method still outputs random guess result. This is mainly due to the inaccurate modeling of the DCT coefficients with the Laplacian distribution. Indeed, even the best fitting Laplacian often has a large fitting error to the ground truth histogram, as illustrated in Fig. 2. This error induced by model inaccuracy has important negative impact on the final forensic result. Luo’s original method also has poor results, providing accuracy of about 60%. The corresponding improved version in general performs slightly better, but the accuracy still remains very low. One possible explanation is that in Luo’s method only two specific and very small ranges of DCT coefficients are considered, which do not necessarily provide discriminative information for JPEG-100 forensics.

The significant performance improvement of our method shown in Table 1 highlights the importance of choosing the histogram bin width equal to 0.5 and the high accuracy of GGD. The new research line that we have proposed in Section II for JPEG-100 forensics, *i.e.*, testing between two candidate distributions which one describes better the given data, also play an important role in achieving this good performance. Our method provides results close to perfect classification (very close to 100% accuracy), and thus fulfills our objective in this paper, *i.e.*, the proposed histogram-based method



(a) D_{I44} and its best fittings



(b) Y_{44}^* and its best fittings

Fig. 6. For UCID00001, we show histogram of D_{I44} in (a) and that of Y_{44}^* in (b), along with their best fitting histograms of GGD and perturbed “discrete” GGD.

Table 1. The accuracy for JPEG-100 forensics, “Imp.” stands for “Improved”.

Subband	Fan’s	Imp. Fan’s	Luo’s	Imp. Luo’s	Ours
(2, 2)	50.00%	50.00%	54.48%	62.33%	98.77%
(4, 4)	50.00%	50.00%	56.05%	64.31%	98.95%
(5, 5)	50.00%	50.00%	56.61%	65.96%	98.95%
(6, 6)	50.00%	50.00%	58.07%	62.74%	99.03%
(8, 8)	50.00%	50.00%	63.68%	57.47%	98.80%

should be able to perform at least comparably with regard to recompression-based methods. In the future, we plan to conduct detailed quantitative comparisons with recompression-based methods. Nevertheless, it is worth pointing out that DCT histogram-based methods perform forensic analysis solely on the given image without any preprocessing like recompression, therefore they appear to be both conceptually and algorithmically simpler and more efficient.

VI. CONCLUSIONS AND FUTURE WORK

This paper has presented a JPEG-100 forensic method based on histogram fitting and distribution identification. It is worth noting that the proposed forensic method has the potential to be a generic one and applied to other forensic problems as long as the task is to discriminate between two parametric distributions. Preliminary experimental results have shown that this novel method works effectively and significantly improves the forensic performance comparing to existing histogram-based methods. This improvement is mainly due to the fact that the GGD describes well the distribution of DCT coefficients and that the histogram is constructed with an appropriate bin width equal to 0.5.

Future work shall be devoted to deriving a better statistical model of the DCT coefficient perturbation, *i.e.*, the probability $p_{Y^*|Y}(Y^* | Y = kq)$ in Eq. (7) in the hope of enhancing the accuracy of JPEG-100 identification. We also plan to develop an algorithm for quantization step estimation for general-purpose JPEG forensics of arbitrary quality factor. More specifically, we jointly optimize α , β and q in Eq. (13) for the perturbed “discrete” GGD. This is an interesting and promising working direction because according to a recent

study there is still much room for improving the estimation accuracy of quantization step under arbitrary quality factor [5].

ACKNOWLEDGMENT

This work is supported in part by the AGIR (Alpes Grenoble Innovation Recherche) project TAFFI.

REFERENCES

- [1] H. Farid, “Digital image ballistics from JPEG quantization: A followup study,” Tech. Rep. TR2008-638, Dartmouth College, Computer Science, 2008.
- [2] J. He, Z. Lin, L. Wang, and X. Tang, “Detecting doctored JPEG images via DCT coefficient analysis,” in *European Conference on Computer Vision, Part III*, pp. 423–435, 2006.
- [3] Z. Fan and R. L. De Queiroz, “Identification of bitmap compression history: JPEG detection and quantizer estimation,” *Image Processing, IEEE Transactions on*, vol. 12, no. 2, pp. 230–235, 2003.
- [4] S. Lai and R. Bohme, “Block convergence in repeated transform coding: JPEG-100 forensics, carbon dating, and tamper detection,” in *Acoustics, Speech and Signal Processing (ICASSP), 2013 IEEE International Conference on*, pp. 3028–3032, IEEE, 2013.
- [5] B. Li, T.-T. Ng, X. Li, S. Tan, and J. Huang, “Revealing the trace of high-quality JPEG compression through quantization noise analysis,” *Information Forensics and Security, IEEE Transactions on*, vol. 10, no. 3, pp. 558–573, 2015.
- [6] B. Li, T.-T. Ng, X. Li, S. Tan, and J. Huang, “Statistical model of JPEG noises and its application in quantization step estimation,” *Image Processing, IEEE Transactions on*, vol. 24, no. 5, pp. 1471–1484, 2015.
- [7] W. Luo, J. Huang, and G. Qiu, “JPEG error analysis and its applications to digital image forensics,” *Information Forensics and Security, IEEE Transactions on*, vol. 5, no. 3, pp. 480–491, 2010.
- [8] G. Schaefer and M. Stich, “Ucid: an uncompressed color image database,” in *Electronic Imaging*, pp. 472–480, International Society for Optics and Photonics, 2003.
- [9] F. Muller, “Distribution shape of two-dimensional DCT coefficients of natural images,” *Electronics Letters*, vol. 29, no. 22, pp. 1935–1936, 1993.
- [10] G. S. Yovanof and S. Liu, “Statistical analysis of the DCT coefficients and their quantization error,” in *Signals, Systems and Computers, 1996. Conference Record of the Thirtieth Asilomar Conference on*, vol. 1, pp. 601–605, IEEE, 1996.
- [11] W. Fan, K. Wang, F. Cayre, and Z. Xiong, “JPEG anti-forensics with improved tradeoff between forensic undetectability and image quality,” *Information Forensics and Security, IEEE Transactions on*, vol. 9, no. 8, pp. 1211–1226, 2014.
- [12] M. C. Stamm and K. R. Liu, “Anti-forensics of digital image compression,” *Information Forensics and Security, IEEE Transactions on*, vol. 6, no. 3, pp. 1050–1065, 2011.
- [13] K. Meshgi and S. Ishii, “Expanding histogram of colors with gridding to improve tracking accuracy,” in *Machine Vision Applications (MVA), 2015 14th IAPR International Conference on*, pp. 475–479, IEEE, 2015.